Study of water diffusion on single-supported bilayer lipid membranes by quasielastic neutron scattering



2012 EPL 98 48006

(http://iopscience.iop.org/0295-5075/98/4/48006)

A Letters Journal Exploring the Frontiers of Physics

May 2012

EPL, **98** (2012) 48006
doi: 10.1209/0295-5075/98/48006

www.epljournal.org

# Study of water diffusion on single-supported bilayer lipid membranes by quasielastic neutron scattering

M. Bai[1], A. Miskowiec[1], F. Y. Hansen[1(a)], H. Taub[1(b)], T. Jenkins[2], M. Tyagi[2,3], S. O. Diallo[4], E. Mamontov[4], K. W. Herwig[4] and S.-K. Wang[1(c)]

[1] *Department of Physics and Astronomy and University of Missouri Research Reactor, University of Missouri Columbia, MO 65211, USA*
[2] *Center for Neutron Research, National Institute of Standards and Technology - Gaithersburg, MD 20899-6102, USA*
[3] *Department of Materials Science and Engineering, University of Maryland - College Park, MD 20742, USA*
[4] *Spallation Neutron Source, Oak Ridge National Laboratory - Oak Ridge, TN 37831, USA*

received 27 March 2012; accepted 23 April 2012
published online 28 May 2012

PACS 87.16.D- – Membranes, bilayers, and vesicles
PACS 78.70.Nx – Neutron inelastic scattering
PACS 87.16.dj – Dynamics and fluctuations

**Abstract** – High-energy-resolution quasielastic neutron scattering has been used to elucidate the diffusion of water molecules in proximity to single bilayer lipid membranes supported on a silicon substrate. By varying sample temperature, level of hydration, and deuteration, we identify three different types of diffusive water motion: bulk-like, confined, and bound. The motion of bulk-like and confined water molecules is fast compared to those bound to the lipid head groups (7–10 $H_2O$ molecules per lipid), which move on the same nanosecond time scale as H atoms within the lipid molecules.



The structure and dynamics of the water associated with lipid membranes and their effect on the functioning of membrane-embedded proteins involve some of the most fundamental issues in biological physics today. For over four decades, Nuclear Magnetic Resonance (NMR) has been used to study the dynamics of membrane-associated water [1–6]. NMR allows investigation of the motion of water molecules on time scales in the ranges $10^{-9}$–$10^{-11}$ s [3,4] and $\sim 10^{-6}$ s [4]. It has been used to demonstrate different freezing points of water, depending on its location with respect to the lipid head groups [1,2]. Quasielastic Neutron Scattering (QENS), with its sensitivity to the motion of H atoms, has proved to be a complementary technique for studying the dynamics of membrane-associated water on time scales in the $10^{-9}$–$10^{-13}$ s range [4,7–11]. It has the advantage that the lipid molecular motion can also be investigated. In addition, the wave vector ($Q$) dependence of the scattering can be used to infer the length scale of both water and lipid motion and to distinguish between types of diffusive motion such as translational, rotational, and conformational.

Most NMR investigations of membrane-associated water have been conducted on multilamellar membrane systems such as lecithin dispersions [1,2] and DMPC powders [5]. QENS measurements have used larger samples usually consisting of stacks of a thousand or more membranes supported on a solid substrate in order to build up sufficient scattered neutron intensities [4,7–12]. Unfortunately, the multilamellar samples used in both NMR and QENS experiments are difficult to model in Molecular-Dynamics (MD) simulations. Besides the sheer number of membranes, the interactions between them within a stack, and the presence of unknown amounts of water between membranes complicate computer simulations of these samples. In the absence of simulations, most QENS measurements have been interpreted assuming just two types of water, bulk-like and membrane-bound, and have been analyzed using simple analytical models of molecular rotation and translation [4].

As an alternative to measurements on multilamellar membrane samples, we report here QENS measurements from membrane-associated water on well-characterized samples of single-supported bilayer lipid membranes as

(a) Permanent address: Department of Chemistry, Technical University of Denmark, IK 207 DTU - DK-2800 Lyngby, Denmark, EU.
(b) E-mail: taubh@missouri.edu
(c) Permanent address: Comprehensive Cancer Center - Palm Springs, CA 92263, USA.

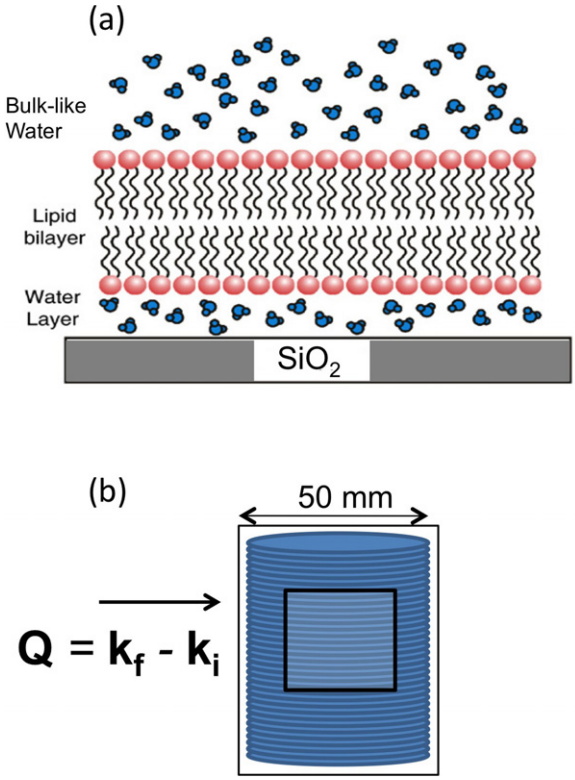


Fig. 1: (Colour on-line) (a) Sketch of a hydrated single-supported bilayer membrane as suggested by ref. [15]. (b) Schematic diagram of the neutron scattering sample consisting of a stack of Si(100) wafers, indicating the direction of the neutron wave vector transfer $\mathbf{Q} = \mathbf{k}_f - \mathbf{k}_i$ parallel to the wafer plane. The square outline indicates the size of the neutron beam incident on the sample.

depicted in fig. 1(a). We were motivated to try such experiments by our recent QENS measurements on pure alkane films with H-atom concentrations comparable to those of single-supported bilayer membranes [13]. The high counting rates of state-of-the-art backscattering spectrometers and the use of large substrates consisting of a stack of 100 single-crystal silicon wafers (see fig. 1(b)) allowed acquisition of QENS spectra on nanometer-thick alkane films in reasonable counting times. Samples of this design have also been used in recent QENS measurements investigating lipid diffusion in single-supported membranes [14].

By using two complementary state-of-the-art backscattering spectrometers, we have been able to probe diffusive motion of water in proximity to single-supported bilayer lipid membranes of DMPC (1,2-dimyristoylsn-glycero-3-phosphocholine) to obtain the following principal results. From the dependence of the QENS spectra on temperature, we present model-independent evidence of two different types of diffusive motion of the membrane-associated water: bulk-like and confined. In addition, we observe a much weaker contribution to the QENS due to a slower motion of H atoms that occurs on a nanosecond time scale. Intensity analysis of this component is consistent with a third type of water, termed "bound," that diffuses on this slower time scale.

Our samples of single-supported DMPC membranes were made by vesicle fusion process [14,15]. The substrate consisted of a cylindrical stack of about 100 acid-cleaned, electronic-grade Si(100) wafers (5 cm diameter, 0.3 mm thick, and polished on both sides) as shown in fig. 1(b) [13]. DMPC ($C_{36}H_{72}NO_8P$) from Avanti Polar Lipids[1] was added to a buffer solution and sonicated at 45 °C for ∼24 h to produce unilamellar vesicles. After deposition of the DMPC, the wafers were rinsed in distilled water to remove additional membrane layers and dried in $N_2$ gas. The wafer stack was loaded into an aluminum cell sealed with an indium O-ring under an argon atmosphere. The hydration level of the membranes could be varied by annealing the samples in an oven at 328 K prior to loading them in the aluminum sample cell and by introducing a water droplet into the sample can before sealing.

Topographic images recorded by Atomic Force Microscopy (AFM) from similarly prepared samples under a flow of moist air show homogeneous membranes with few holes or cracks [16]. The membranes had a typical thickness of ∼6.3 nm at room temperature which is somewhat larger than the ∼4.6 nm reported from neutron reflectivity measurements on single-supported DMPC membranes submerged in $D_2O$ [17]. In our AFM measurements, we observe a decrease in the membrane thickness to ∼5.2 nm over the temperature range 308–328 K, which we interpret as a broadened gel-to-fluid transition that has been shifted upward in temperature. We suggest that the larger thicknesses of these single-supported membranes as measured by AFM may be explained by the out-of-plane disorder of the lipid molecules found in MD simulations on freestanding membranes [18]. This disorder is parameterized as roughness of the membrane in modeling the reflectivity curves but could contribute to the thickness of the membrane when measured with a nanoscale AFM probe.

In fig. 2, we show the temperature dependence of the intensity of neutrons elastically scattered from a sample of single-supported DMPC membranes as measured on the High-Flux Backscattering Spectrometer (HFBS) at the NIST Center for Neutron Research [19]. This "wet" sample was prepared by first annealing it in air for 72 h at a temperature of 328 K before sealing the wafer stack in the sample can with 120 $\mu$l of $H_2O$ to ensure full hydration of the membranes. The elastic intensity in fig. 2 has been summed over all wave vector transfers and measures the number of neutrons scattered with energy transfers less than ∼1 $\mu$eV, the full width at half maximum (FWHM) of the HFBS' resolution function. Because incoherent scattering from the hydrogen atoms dominates the elastic signal, a decrease in elastic intensity

[1]Certain commercial equipment, instruments, or materials (or suppliers) are identified in this paper to foster understanding. Such identification does not imply recommendation or endorsement by the National Institute of Standards and Technology, nor does it imply that the materials or equipment identified are necessarily the best available for this purpose.

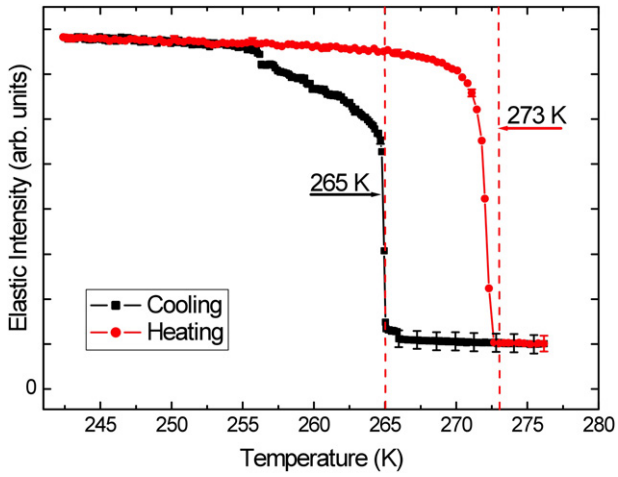


Fig. 2: (Colour on-line) Elastic intensity measured on the backscattering spectrometer (HFBS) at NIST while cooling (squares (black)) and heating (circles (red)) the "wet" single-supported DMPC membrane sample (see text). Error bars in the figures represent one standard deviation.

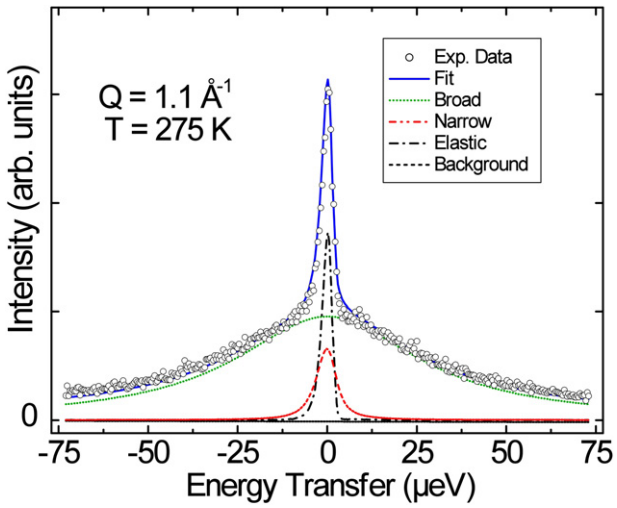


Fig. 3: (Colour on-line) Typical spectrum measured on BASIS from the "wet" single-supported DMPC membrane sample at $Q = 1.1\,\text{Å}^{-1}$ and a temperature of 275 K. The data points are the open circles. The spectrum has been fit to a scattering law composed of three terms: a delta function corresponding to the elastic scattering plus two Lorentzians representing the quasielastic scattering. The best fit shown by the solid (blue) line is obtained after folding each of these terms with the instrumental resolution function. It has three components: 1) the "broad" Lorentzian shown by the dotted (green) line contributed by the bulk-like water; 2) the "narrow" Lorentzian (FWHM ∼5.0 $\mu$eV) shown by the dash–double-dotted (red) line identified with slower motions associated with conformational changes of the lipid tails; and 3) the elastic component shown by the dash-dotted (gray) line. The darker dashed (black) line indicates the linear background level.

measures the number of H atoms in the sample moving on a time scale faster than ∼1 ns. We shall see that for the "wet" sample in fig. 2, most of the H atoms are in the $H_2O$ molecules. Therefore, at low temperatures, water provides the dominant contribution to the elastic intensity. At temperatures above 273 K where the elastic intensity levels off at its lowest value, the motion of H atoms in both water and membrane are faster than the time scale of the instrument so that the elastic scattering is contributed by the silicon substrate.

The elastic intensity plotted in fig. 2 shows a much more abrupt change with temperature than found for the water in samples consisting of membrane stacks [9–11]. On slow heating (0.1 K/min), we see a single, large vertical step downward just below 273 K, the melting point of bulk $H_2O$. It is preceded by a slower decrease in intensity beginning at ∼268 K, indicating the presence of water with a melting point below that of bulk. In contrast, on slow cooling of this sample (0.04 K/min), we observe little change in the elastic intensity until a large step-like increase in the neutron intensity occurs at 265 K, somewhat below the feature at 271 K attributed to the freezing of water in a sample consisting of a stack of thousands of membranes [9]. Despite this large hysteresis, the abrupt intensity increase on cooling indicates a homogeneous sample and the thermal equilibration of the wafer stack. On further cooling, the elastic intensity continues to increase, but more gradually, until it saturates below a temperature of ∼256 K. This behavior suggests that there is still mobile water moving on a nanosecond time scale below the freezing transition at 265 K.

Because the silicon substrate is identical to that used previously in our study of alkane films [13], we can use the increase in elastic intensity measured on cooling of alkane films of known coverage to estimate the number of H atoms in our membrane samples. Allowing for the H atoms in the single DMPC bilayer coating on each side of the 100 silicon wafers, we can calculate the remaining number of H atoms associated with the water in the sample. Assuming the water to have the bulk density, we estimate that this wet sample contains an amount of water equivalent to a slab ∼120 nm thick. We emphasize that the morphology of this water is unknown. While most of it is likely to be located above the lipid head groups in the upper leaflet, we do not have evidence of the water wetting the membrane to form a layer of uniform thickness. It may, in fact, be in the form of bulk droplets.

In order to determine the types of molecular motion responsible for the loss of elastic intensity in the membrane samples, we obtained quasielastic spectra on the backscattering spectrometer BASIS [20] at the Spallation Neutron Source (SNS), Oak Ridge National Laboratory. Using the same wet sample, we obtained spectra every 0.5 K with a counting time of 1 h. We have fit the spectra by folding the instrumental resolution function with a scattering law composed of three terms: a delta function corresponding to the elastic scattering plus two Lorentzians representing the quasielastic scattering. The decomposition of a spectrum into these three components and a linear background term is illustrated in fig. 3. We see that the temperature dependence of the delta-function intensity in fig. 4(a) agrees well

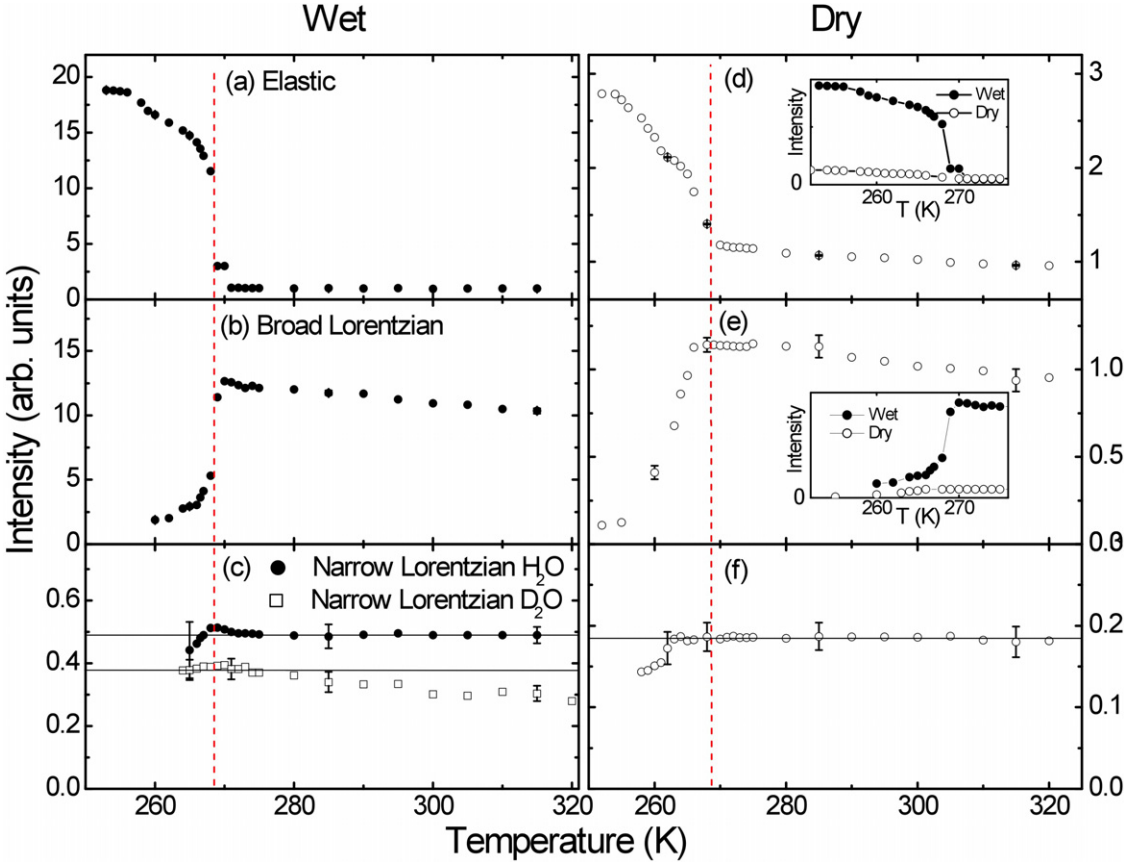


Fig. 4: (Colour on-line) Quasielastic neutron intensity *vs.* temperature as observed from the "wet" single-supported DMPC membrane sample (left panels), using the backscattering spectrometer (BASIS) at the SNS. Measurements were made on cooling in 0.5 K steps, counting 1 h per point. Each panel represents the intensity associated with one of the three terms in the scattering law used to model the spectra: (a) elastic intensity corresponding to the intensity of the delta-function term obtained in a fit to a composite spectrum summed over all $Q$. (b) Integrated intensity of the "broad" Lorentzian fitted to a spectrum summed over wave vector transfers $Q$ of 0.5 Å$^{-1}$, 0.7 Å$^{-1}$, and 0.9 Å$^{-1}$. (c) Integrated intensity of the "narrow" Lorentzian fitted to a spectrum summed over wave vector transfers $Q$ of 1.4 Å$^{-1}$, 1.5 Å$^{-1}$, and 1.7 Å$^{-1}$. Similar data for the "dry" sample (right panels): (d) elastic intensity; (e) integrated intensity of the "broad" Lorentzian component; and (f) integrated intensity for the "narrow" Lorentzian component. Note that the Lorentzian intensities have been normalized to the sample's elastic intensity at high temperature (taken to be unity) thereby allowing comparison of the Lorentzian intensities in the two samples (see text). The vertical dashed lines (red) indicate the freezing temperature of the bulk-like water. In (c) and (f) the solid horizontal lines indicate the intensity assumed in the calculation of the number of water molecules per lipid (see text). Insets in (d) and (e) show relative intensity of the wet and dry samples.

with that of the elastic intensity measured on the HFBS as shown in fig. 2 except that the step-like increase in intensity on cooling now occurs about three degrees higher at 268 K. Generally, we found the temperature at which the intensity step occurred to increase with the first few thermal cycles.

The large dynamic range of BASIS allows us to resolve two diffusive processes occurring at different rates as shown in fig. 3: a "fast" motion (time scale <40 ps) that can be fit to a broad Lorentzian (dotted curve (green)) and a "slow" motion (time scale ∼0.5 ns) described by a narrow Lorentzian (dash–double-dotted curve (red)). The FWHM of the broad Lorentzian has a $Q^2$ dependence at low $Q$ (not shown) characteristic of translational diffusion. Measurements with this wet sample at a temperature of 275 K yield a diffusion constant of $1.02 \times 10^{-5}$ cm$^2$/s close to but smaller than the value of $1.13 \times 10^{-5}$ cm$^2$/s obtained previously for bulk water at this temperature [21]. Therefore, above the step-like increase in the elastic intensity at 268 K (see fig. 4(a)), we identify the broad Lorentzian component with the translational diffusion in "bulk-like" water. Here we use the term "bulk-like" to indicate a diffusion constant close to but somewhat smaller than the bulk value in this temperature range. In the case of the slower motion corresponding to the narrow Lorentzian component that has a ∼5 $\mu$eV FWHM and which is nearly $Q$-independent (not shown), we tentatively identify it with a motion primarily involving conformational changes of the alkyl tails of the lipid molecules. From both QENS measurements and MD simulations, we have found evidence of similar motion in solid bulk alkane particles [13] and in monolayer alkane films [22].

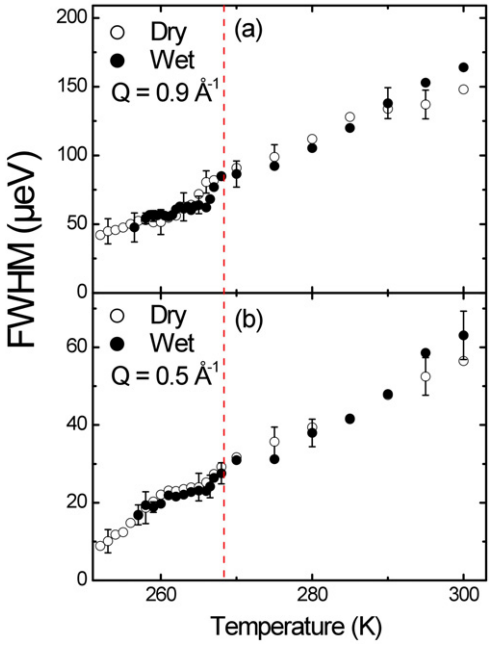


Fig. 5: (Colour on-line) Temperature dependence of the FWHM of the "broad" Lorentzian fit to quasielastic spectra measured on BASIS from the wet sample (solid circles), the dry sample (open circles) at two different wave vector transfers: (a) $Q = 0.9\,\text{Å}^{-1}$; and (b) $Q = 0.5\,\text{Å}^{-1}$. The vertical dashed line (red) indicates the freezing temperature of the bulk-like water.

We next consider the origin of the broad Lorentzian component in the QENS at lower temperatures. In contrast to the intensity of the narrow Lorentzian component that has only a weak temperature dependence (see fig. 4(c)), we see that the intensity of the broad Lorentzian has a step-like decrease at 268 K on cooling (fig. 4(b)) that coincides with the step-like increase in the elastic intensity in fig. 4(a). This behavior is consistent with about 2/3 of the water becoming immobile on a nanosecond time scale. For that reason, we interpret the step at 268 K as the freezing of bulk-like water presumably located above the lipid head groups in the upper leaflet of the membrane.

In order to compare the diffusive motion of the water below the freezing point of the bulk-like water at 268 K with that above, we plot in fig. 5 the temperature dependence of the FWHM of the broad Lorentzian component at two different wave vector transfers: (a) $Q = 0.9\,\text{Å}^{-1}$ and (b) $Q = 0.5\,\text{Å}^{-1}$. At both wave vector transfers, we see a small step-like decrease in the FWHM on cooling just below 268 K. On further cooling, the FWHM appears to decrease more slowly with temperature. We tentatively identify this behavior that differs qualitatively from that of bulk supercooled water [21] with the translational diffusive motion of water *confined* to a region near the head groups. The presence of mobile water below 268 K is also consistent with the gradual increase in the elastic intensity observed on cooling below 268 K.

To investigate the motion of water more tightly bound to the membrane, we performed QENS measurements on single-supported membrane samples of lower hydration. We fabricated a "dry" sample by eliminating both the heating of the deposited membranes to 328 K prior to loading and also the droplet of water in the sample can. To increase sensitivity to the water motion, we used DMPC membranes in which the lipid tails were deuterated ($C_{36}D_{54}H_{18}NO_8P$). For this dry sample, we see in fig. 4(d) that the elastic scattering is now much weaker. From the magnitude of the increase in elastic intensity between the highest and lowest temperatures, we infer that the dry sample has about a factor of ∼10 less water than the wet sample. Although a vertical step in the elastic intensity is no longer visible on cooling to 267 K, we again observe a continuous increase in intensity at lower temperatures that we attribute to mobile water confined to a region near the lipid head groups. In fig. 4(e), one sees a corresponding continuous decrease in the intensity of the broad Lorentzian component on cooling below 268 K.

To compare the rate of the diffusive motion of the water molecules in the wet and dry samples, we have included the FWHM of the broad Lorentzian component for the dry sample in fig. 5. Despite the order of magnitude difference in the amount of water in the two samples, we see that they have essentially the same FWHM over the entire temperature range. In particular, the confined water that remains mobile below the freezing point of the bulk-like water has a translational diffusion rate comparable to that in the wet sample. Above this freezing point, there is apparently still enough bulk-like water in the dry sample for it to dominate the contribution to the QENS.

It is also of interest to compare the intensity of the narrow Lorentzian component in the spectra of the wet and dry samples as shown in figs. 4(c) and (f), respectively. Whereas the wet sample has about a factor of 10 more water in it than the dry sample, the intensity of the narrow Lorentzian component in the wet sample is only about a factor of 2.7 larger than that for the dry sample. This disparity supports our tentative interpretation of the narrow Lorentzian as originating primarily in motion of the lipid molecules rather than from the water in the samples. Furthermore, if the motion were to be confined to the lipid tails, then we would expect a much weaker narrow Lorentzian component for the dry sample because of the complete deuteration of its alkyl chains. For this reason, we have considered the possibility that the H atoms in the head groups also move on the slower time scale that we have identified with conformational changes in the lipid tails [13]. This interpretation is supported by calculations of the diffusion rate of selected atoms in the head groups in recent MD simulations [18]. Including all 72 H atoms in the lipid molecules of the wet sample and the 18 H atoms in the head groups of the dry sample (the tails were deuterated), gives an H atom ratio of $72/18 = 4$ compared to the ratio of 2.7 for the narrow Lorentzian intensities in the two samples. However, if we assume that there are also $H_2O$ molecules bound to the lipid head groups strongly enough that they also participate in this slower motion, we can fit the observed narrow Lorentzian intensity ratio of 2.7 by

assuming $\sim 7\,H_2O$ molecules per head group. By applying a similar analysis to the ratio of the narrow Lorentzian intensity in the wet sample to that in a third sample of protonated membranes hydrated with $D_2O$ to the same level as the wet sample (see fig. 4(c)), yields the estimate of $\sim$10 water molecules bound per lipid head group. Finally, analyzing the ratio of intensities for the dry and wet ($D_2O$) samples, yields as estimate of $\sim$8 bound water molecules. This range of 7−10 bound water molecules per lipid head group in single-supported membranes can be compared with values of 9.7 and $4.3\,D_2O$ molecules per head group obtained from NMR experiments on multilamellar DMPC membranes in their fluid and gel phases, respectively [5]. A similar analysis of quasielastic spectra calculated from MD simulations of freestanding membranes in a fluid phase at a temperature of 303 K gives an estimate of 5−6 water molecules per lipid [18].

Due to possible differences in structure between our single-supported membranes and freestanding membranes, some caution is needed in comparing these values for the number $N$ of water molecules bound per lipid head group. For example, our intensity analysis of the narrow Lorentzian component in the QENS spectra has assumed the same $N$ for both leaflets of a single-supported membrane. If the effect of the substrate were to decrease the number of bound water molecules in the lower leaflet [16], then our analysis would give a larger value of $N$ in the upper leaflet than estimated above. Also, the stability of the gel phase up to $\sim$320 K that we observe in similarly prepared samples [16] may indicate a lattice constant of the membrane and a tilt angle of the lipid molecules differing from that of a freestanding membrane.

In summary, the following picture of the diffusive motion of water emerges from our QENS measurements on single-supported bilayer lipid membranes. Our wet and dry samples differ principally in the amount of bulk-like water present above the membrane. For both samples, the QENS from this bulk-like water dominates the spectra above its freezing temperature. Below this temperature, we find evidence of "confined" water whose translational diffusion rate exhibits a temperature dependence differing qualitatively from that of bulk supercooled water. All samples exhibit evidence of a slower diffusive motion of water that we attribute to molecules bound to the lipid head groups and moving on the same nanosecond time scale as the H atoms within the lipid molecules.

* * *

This work was supported by the U.S. National Science Foundation under Grant Nos. DMR-0705974 and DGE-1069091 and utilized facilities supported in part by the NSF under agreement No. DMR-0944772. A portion of this research at Oak Ridge National Laboratory's Spallation Neutron Source was sponsored by the Scientific User Facilities Division, Office of Basic Energy Sciences, U.S. Department of Energy. We thank Dan A. Neumann and Ioan Kosztin for helpful discussions.

REFERENCES

[1] Salsbury N. J., Darke A. and Chapman D., *Chem. Phys. Lipids*, **8** (1972) 142.
[2] Finer E. G., *J. Chem. Soc., Faraday Trans.*, **69** (1973) 1590.
[3] Bayerl T. M. and Bloom M., *Biophys. J.*, **58** (1990) 357.
[4] König S., Sackmann E., Richter D., Zorn R., Carlile C. and Bayerl T. M., *J. Chem. Phys.*, **100** (1994) 3307.
[5] Faure C., Bonakdar L. and Dufourc E. J., *FEBS Lett.*, **405** (1997) 263.
[6] Kausik R. and Han S., *Phys. Chem. Chem. Phys.*, **13** (2011) 7732.
[7] Pfeiffer W., Henkel Th., Sackmann E., Knoll W. and Richter D., *Europhys. Lett.*, **8** (1989) 201.
[8] König S., Pfeiffer W., Bayerl T., Richter D. and Sackmann E., *J. Phys. II*, **2** (1992) 1589.
[9] Rheinstädter M. C., Seydel T., Demmel F. and Salditt T., *Phys. Rev. E*, **71** (2005) 061908.
[10] Swenson J., Kargi F., Bernsten P. and Svanberg C., *J. Chem. Phys.*, **129** (2008) 045101.
[11] Trapp M., Gutberlet T., Juranyi F., Unruh T., Demé B., Tehei M. and Peters J., *J. Chem. Phys.*, **133** (2010) 164505.
[12] Sackmann E, *Science*, **271** (1996) 43; Tanaka M. and Sackmann E., *Nature*, **437** (2005) 656.
[13] Wang S.-K., Mamontov E., Bai M., Hansen F. Y., Taub H., Copley J. R. D., García Sakai V., Gasparovic G., Jenkins T., Tyagi M., Herwig K. W., Neumann D., Montfrooij W. and Volkmann U. G., *EPL*, **91** (2010) 66007.
[14] Armstrong C. L., Kaye M. D., Zamponi M., Mamontov E., Tyagi M., Jenkins T. and Rheinstädter M. C., *Soft Matter*, **6** (2010) 5864.
[15] Castellana E. T. and Cremer P. S., *Surf. Sci. Rep.*, **61** (2006) 429.
[16] Bai M., Miskowiec A., Schnase P., King G., Hansen F. Y. and Taub H., *Study of single-supported DMPC lipid bilayer membranes as a function of hydration level using neutron reflectivity and atomic force microscopy*, in preparation.
[17] Johnson S. J., Bayerl T. M., McDermott D. C., Adam G. W., Rennie A. R., Thomas R. K. and Sackmann E., *Biophys. J.*, **59** (1991) 289.
[18] Hansen F. Y., Peters G. H., Taub H. and Miskowiec A., *Diffusion of water and selected atoms in DPMC lipid bilayer membranes*, submitted to *J. Chem. Phys.*
[19] Mayer A., Dimeo R., Gehring P. and Neumann D., *Rev. Sci. Instrum.*, **74** (2003) 2759.
[20] Mamontov E. and Herwig K. W., *Rev. Sci. Instrum.*, **82** (2011) 085109.
[21] Teixeira J., Bellissent-Funel M.-C., Chen S. H. and Dianoux A. J., *Phys. Rev. A*, **31** (1985) 1913.
[22] Hansen F. Y., Criswell L., Fuhrmann D., Herwig K. W., Diama A., Dimeo R. M., Neumann D. A., Volkmann U. G. and Taub H., *Phys. Rev. Lett.*, **92** (2004) 046103; Enevoldsen A. D., Hansen F. Y., Diama A., Taub H., Dimeo R. M., Neumann D. A. and Copley J. R. D., *J. Chem. Phys.*, **126** (2007) 104704.